Supplementary Figure Legends

Supplementary Figure S1. ASH response to glycerol changes in lethargus independent of indicator expression. (A) Average Response 1M glycerol as measured by GCaMP3 in the ASH. Lethargus (n=25) and young adult (n=18). **(B)** Quantification of YFP and CFP expression in the ASH neuron of ASH::YC2.12 of one animal over time. **(C)** Quantification of baseline YFP/CFP ratio and amount of peak increase in ratio in response to 1mM Cu^{2+} in the ASH neuron of the same ASH::YC2.12 animal measured in **B**. Related to Figure 1.

Supplementary Figure S2. Calcium concentrations show minimal fluctuations during lethargus and occur consistently and robustly only in the presence of a stimulus.
(A) AVA activity was measured by ratiometric FRET imaging. Representative individual traces are shown. The signal was calculated as the ratio of YFP to CFP emission at each time point. Intrinsic activity was measured during the 30s interval, and there are discernable calcium transients in the L4 worms. **(B)** AVA activity measured in individual worms over time. Intrinsic activity was measured during the 30s interval longitudinally as the worms went into and came out of lethargus. **(C)** Image of the neurons in which GCaMP3 was measured. ASH is marked by the presence of both GCaMP3 and mCherry, AVD is posterior (white arrow), and AVA is anterior (white arrowhead). **(D)** Representative traces of a glycerol trial in a single animal and representative traces of the control buffer trial. **(E)** Heat map of 60s trials denoting influx (red) and efflux (blue) in glycerol (n=18) and buffer (n=14). The proportion of influx or efflux were averaged across trials in 1s bins and are denoted by the gray bars above the heat maps. Related to Figure 2.

Supplementary Figure S3. Regional illumination can elicit changes in calcium concentration in the cell body. (A,C) Images of the neurons in which regional illumination of the cilia was performed and sensory response at the cell body was

measured. **(B,D)** Light contamination at the cell body was measured with varying illumination at the cilia. **(E)** GCaMP3 measurements at ASH cell body in response to ChR2 activation at the cilia. The GCaMP3 change is fluorescence is not significant between the lethargus and young adult (n=8). Related to Figure 3.

Supplementary Figure S4. AVA response to ChR2 decreases significantly despite a lack of corresponding difference in ChR2 expression in AVA during lethargus. (A) Image of the *pnmr-1::ChR2::mcherry* expression (left=*mcherry*, middle= DIC, right= overlay). Expression is seen in 3 sets of neurons (AVA, AVD, and AVE). Scale bar is 20μm. **(B)** Quantification of ChR2::mcherry expression in AVA, AVD, AVE of the *nmr-1* animals during L4, lethargus, and young adult. The mean ± s.e.m. values are shown: L4 (n=5), lethargus (n=5), *p<0.05, ANOVA. **(C)** Quantification of the ratio of ChR2::mcherry expression in the AVD and AVA of *nmr-1* animals during L4, lethargus, and young adult. The mean ± s.e.m. values are shown: L4 (n=5), lethargus (n=5), *p<0.05, Student's t-test of unequal variance. **(D)** Quantification of ChR2::GFP expression in AVA of the ZX1020 animals during L4, lethargus, and young adult. The mean ± s.e.m. values are shown: L4 (n=10), lethargus (n=11), young adult (n=13), NS, ANOVA. **(E)** Depolarization of AVA with RIG showed a significant delay in lethargus (n=22) when compared with L4 (n=17) and adult (n=9); ***p<0.0001, ANOVA. All ATR treated animals were compared to their paired non-ATR treated controls L4 (n=15), lethargus (n=15), adult (n=9); p<0.0001, Student's t-test of unequal variance. **(F)** Depolarization of AVA with RIM also showed a significant delay in lethargus (n=17) when compared with L4 (n=15) and adult (n=8); ***p<0.0001, ANOVA. All ATR treated animals were compared to their paired non-ATR treated controls L4 (n=15), lethargus (n=14), adult (n=8); p<0.0001, Student's t-test of unequal variance. **(G)** Distribution of individual trials show two different populations during lethargus, making reversal behavior in lethargus significantly different; ***p<0.0001, MannWhitney test. **(H)** Distribution of individual trials show two different populations during lethargus, making reversal

behavior in lethargus significantly different; ***p<0.0001, MannWhitney test. Related to Figure 4.

Supplementary Figure S5. Changing activation thresholds introduce delays in the circuit. (A) Schematic of the feed forward loop. Equations from the model were adapted from those published in (Kashtan et. Al 2005). **(B)** Simulation of dynamics built from the equations shown in (A). Threshold at ASH and AVD are adjusted to illustrated changes in dynamics at the downstream neurons. Input values were entered at I=1 and I=0.5. Previous published values for α=1 and β=1 (Kashtan et al., 2004). Related to Figure 5.

Supplementary Figure S6. ASH sensory neurons require increased stimulation to suppress lethargus behavior and this change in threshold is likely both a general sensory phenomena and can be modified by prior activity. (A) Behavioral response to graded intensity of optical stimulation of ChR2 in L4, lethargus and young adult animals at 100μM and 1mM concentrations. **(B)** Reversal following light activation of the ASH neuron in animals grown on 10μM ATR as compared to no ATR control and *lite-1* grown on 10μM ATR. The mean ± s.e.m. values are shown: L4 (n=9), lethargus (n=12), adult (n=8), ***p=0.0001, ANOVA. **(C)** Control behavioral response to graded intensity of optical stimulation of ChR2 in L4, lethargus, and young adult animals at 100μM ATR concentration. The mean ± s.e.m. values are shown: L4 (n=19), lethargus(n=12), adult (n=8), NS, ANOVA. **(D)** Control behavioral response to graded intensity of optical stimulation of ChR2 in L4, lethargus, and young adult animals at 1mM ATR concentration. The mean ± s.e.m. values are shown: L4 (n=9), lethargus(n=7), adult (n=8), NS, ANOVA. **(E)** Response time to ASH::ChR2 in animals that had previously been perturbed during lethargus. L4 (n=10), lethargus unperturbed (n=19), lethargus perturbed (n=25). **(F)** Representative traces of Cameleon measurements in the young adult and lethargus ASEL sensory neuron in response to 80mM NaCl. Related to Figure 6.

Supplementary Movies.

Movies. ZX1020 lethargic animals were followed with low intensity halogen light in an open loading area of the microfluidic chamber. The region of the AVA was previously identified and was selected for illumination. Chr2 in this strain is fused to GFP and signal from the activated region can be seen in real time. The stimulation duration is 10s and begins 10s into the trial to measure the basal rate of activity, and the following 30s was followed. **Movie S1**. Delayed response. **Movie S2.** Immediate response

Supplementary Figure 1

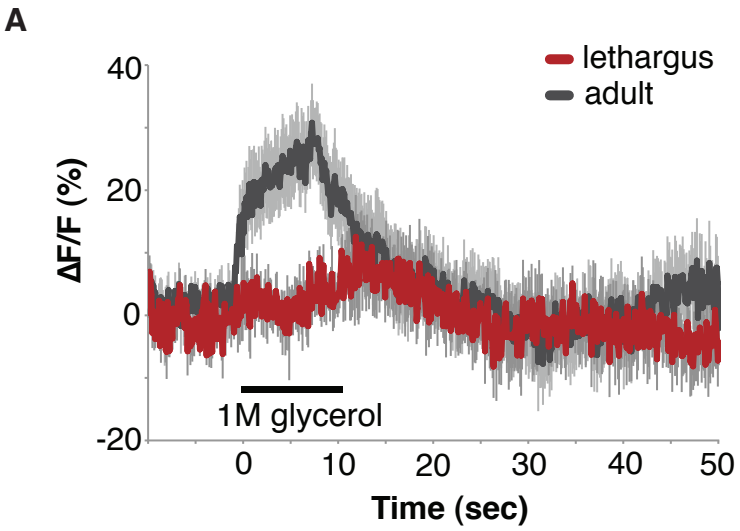

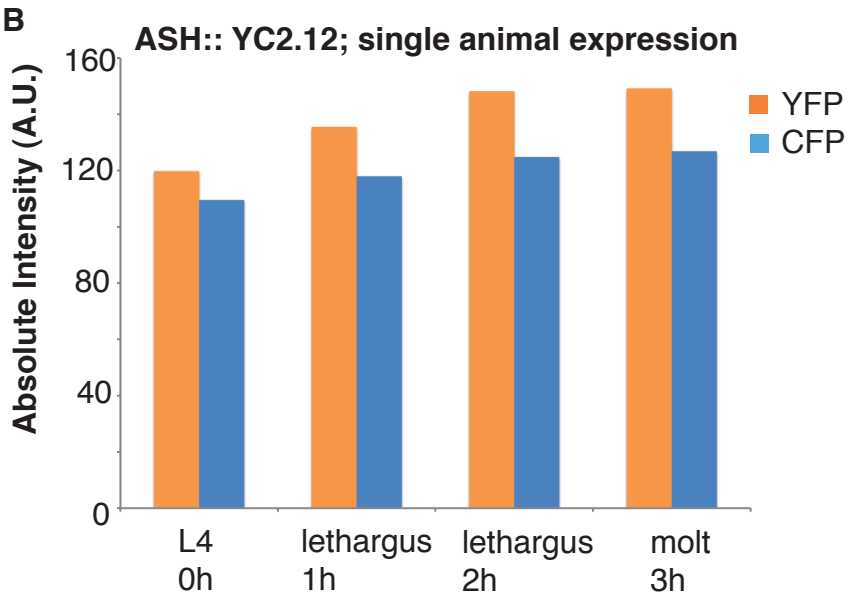

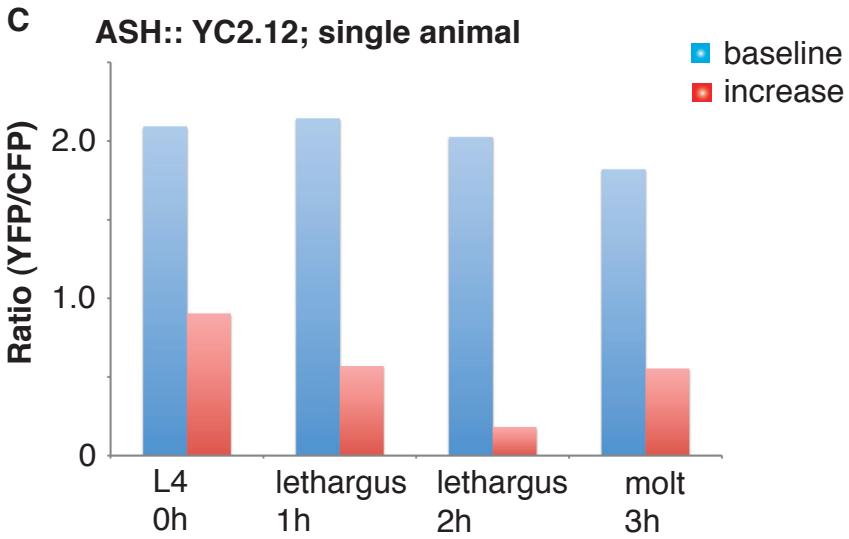

Supplementary Figure 2

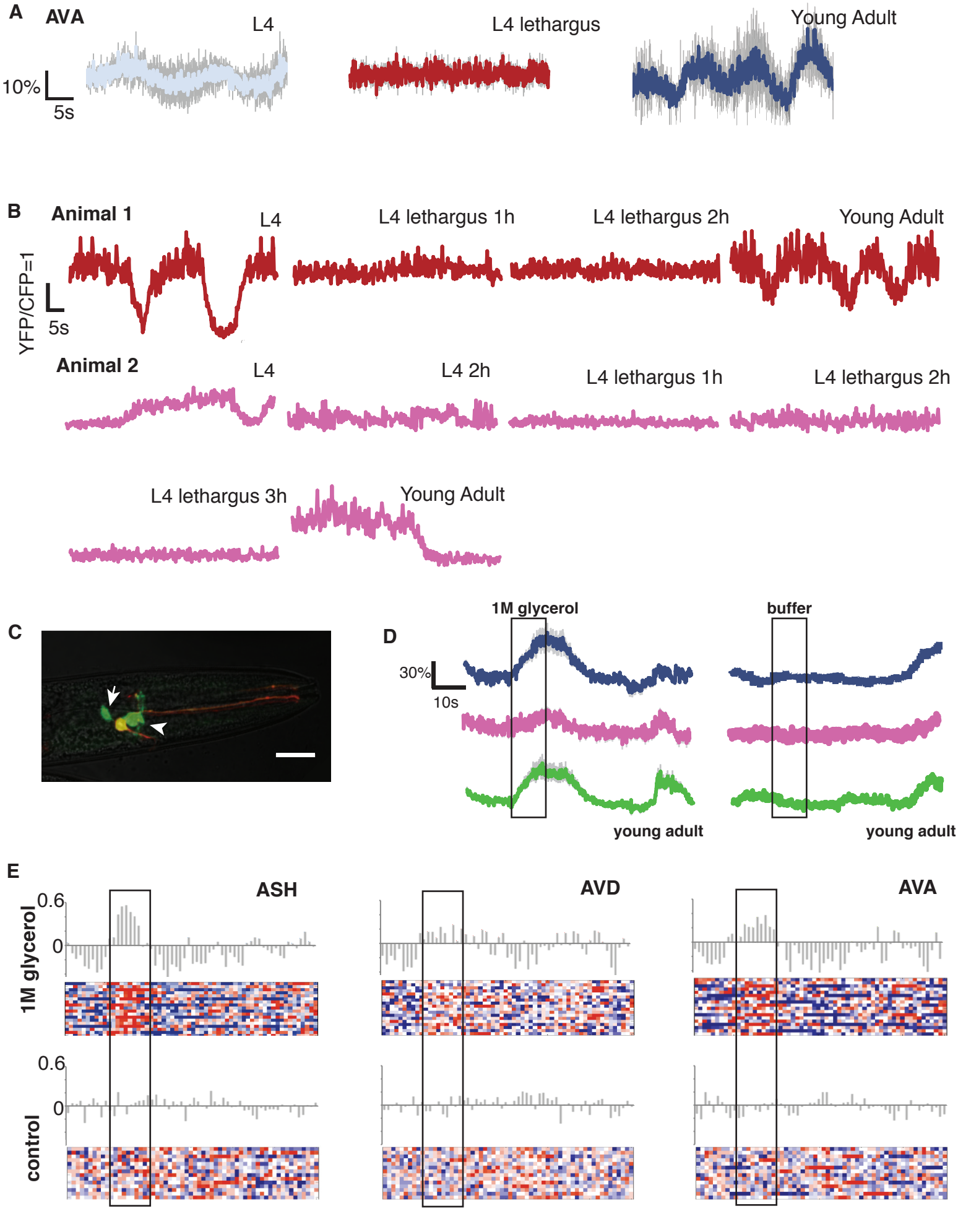

Supplementary Figure S3

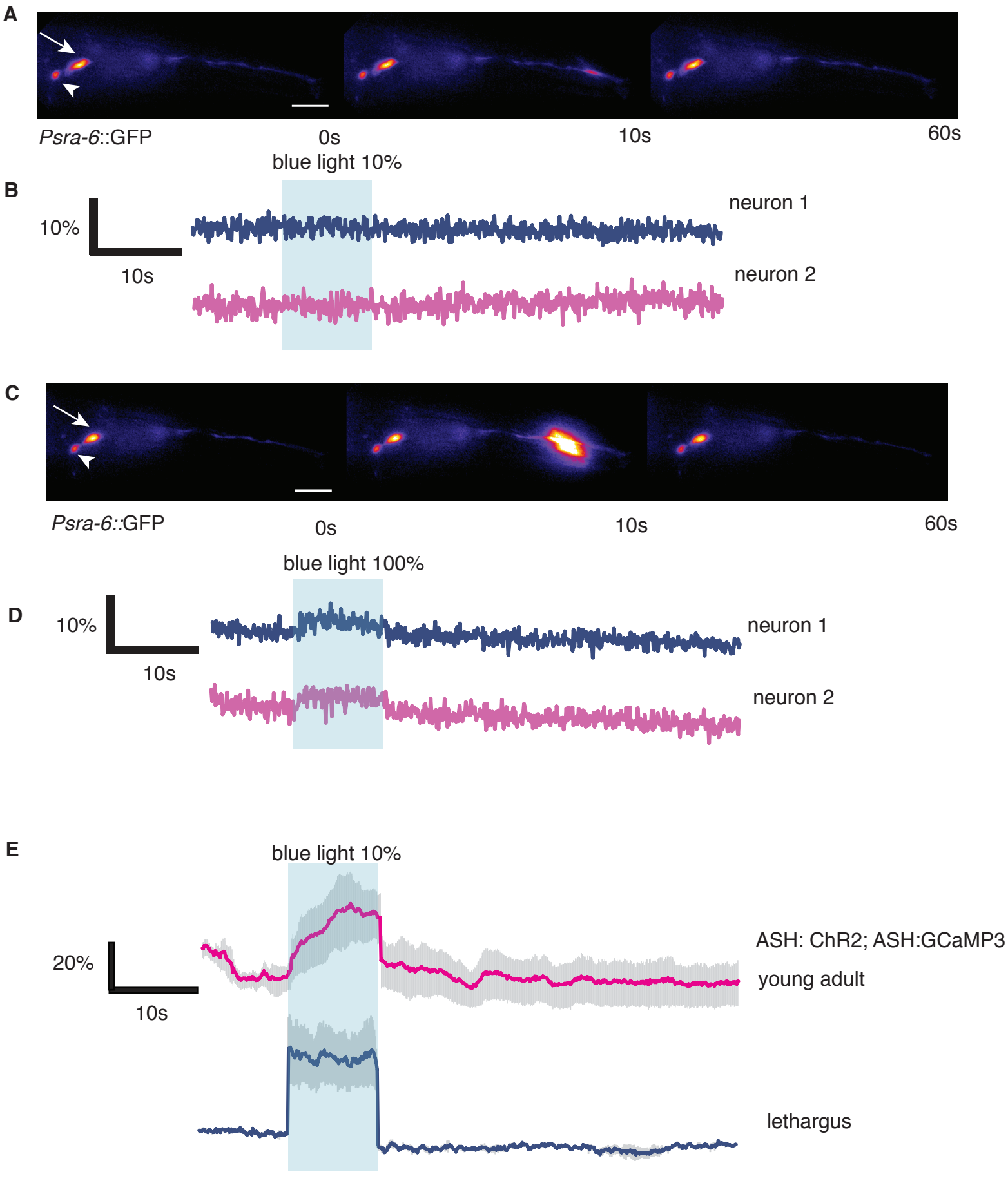

Supplementary Figure S4

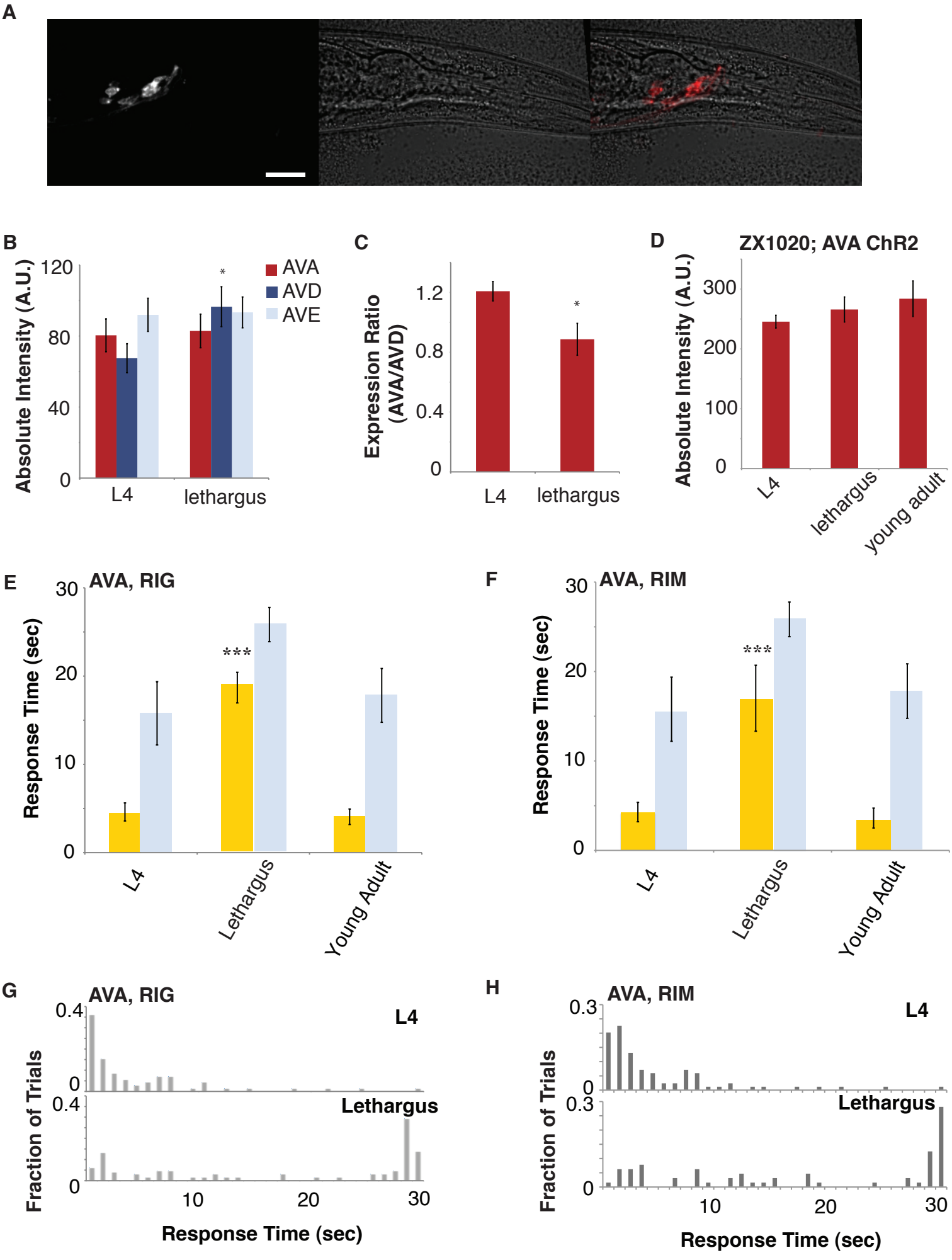

Supplementary Figure S5

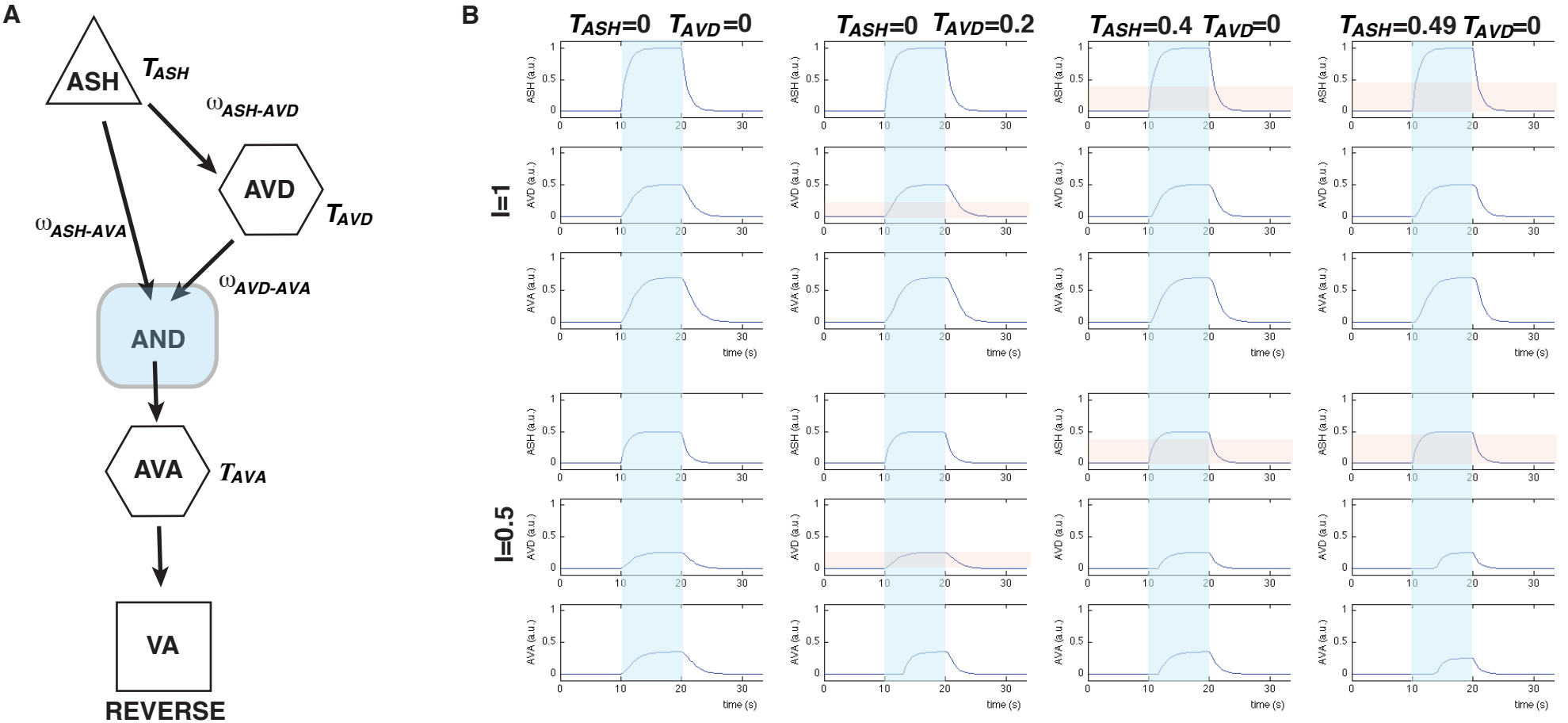

$$dASH/dt = \beta(I > T_{ASH}) - \alpha ASH$$
$$dAVD/dt = \beta(ASH\omega_{ASH\text{-}AVD} > T_{AVD}) - \alpha AVD$$
$$dAVA/dt = \beta(ASH\ \omega_{ASH\text{-}AVA} + AVD\omega_{AVD\text{-}AVA} > T_{AVA}) - \alpha AVA$$
α=1,β=1, ω_i=1

Supplementary Figure S6